A Multivariate Map-Comparison Method for Spatial Evaluation of Model Experiments and Model-Data Comparison — A Synthesis Tool for CMIP-6 Illustrated Using Results from SeaRISE

Ute Herzfeld[1,2,3], Thomas Trantow[1,3], Mattia Astarita[4], Sophie Nowicki[5], Ayako Abe-Ouchi[6], Hyeungu Choi[7], James Fastook[8], Ralf Greve[9], Anders Levermann[10,11,12], Mathieu Morlighem[13, 14], Byron R. Parizek[15], David Pollard[16], Stephen F. Price[17], Fuyuki Saito[18], Hakime Seddik[9], Helene Seroussi[14], Ryan Walker[5,18], and Wei Li Wang[5]

[1]Department of Electrical, Computer and Energy Engineering, University of Colorado Boulder, Boulder, Colorado, USA.
[2]Cooperative Institute for Research in Environmental Sciences, University of Colorado Boulder, Boulder, Colorado, USA.
[3]Department of Applied Mathematics, University of Colorado Boulder, Boulder, Colorado, USA.
[4]Department of Aerospace Engineering, University of Colorado Boulder, Boulder, Colorado, USA.
[5]NASA Goddard Space Flight Center, Greenbelt, Maryland, USA.
[6]Atmosphere and Ocean Research Institute, The University of Tokyo, Kashiwa, Japan.
[7]Sigma Space Corporation, Lanham, Maryland, USA.
[8]Computer Science/Quaternary Institute, The University of Maine, Orono, Maine, USA.
[9]Institute of Low Temperature Science, Hokkaido University, Sapporo, Japan.
[10]Potsdam Institute for Climate Impact Research, Potsdam, Germany.
[11]Lamont Doherty Geological Observatory, Columbia University, New York, USA
[12]Physics Institute, Potsdam University, Potsdam, Germany.
[13]Department of Earth System Science, University of California Irvine, Irvine, California, USA.
[14]Jet Propulsion Laboratory, California Insitute of Technology, Pasadena, California, USA.
[15]Department of Mathematics and Geoscience, Penn State DuBois, DuBois, Pennsylvania, USA.
[16]Earth and Environmental System Institute, The Pennsylvania State University, University Park, Pennsylvania,USA.
[17]Los Alamos National Laboratory, Los Alamos, New Mexico, USA.
[18]Research Institute for Global Change, Japan Agency for Marine-Earth Science and Technology, Yokohama, Japan.
[19]Earth System Science Interdisciplinary Center, University of Maryland, College Park, Maryland, USA.

Correspondence to: Ute Herzfeld (ute.herzfeld@colorado.edu)

Abstract.

Numerical simulations resultant from the Ice Sheet Model Intercomparison Project (ISMIP6), the Sea-Ice Model Intercomparison Project (SIMIP) and other components of the Coupled Model Intercomparison Project 6 (CMIP6) will produce many different spatial variables, from a number of models, a number of experiments and for several scenarios. The typical approaches for analysis of multi-variate multi-model spatial experiment results, or maps, used to date are difference maps or visual comparison based on a pair of the resultant maps or alternatively plots of a summarizing parameter (one value per map) if several maps are involved in a comparison. Here we introduce a multivariate map-comparison method for model evaluation and spatial model-data comparison, that is specifically designed to match the goals and geographic regions of ISMIP6 and SIMIP. The method employs an algebraic semi-norm defined in a space of any finite order over a spatial domain. The map comparison tool MAPCOMP facilitates spatial analysis of results from multi-variate multi-model experiments for any number

of model variables without first reducing the wealth of information from those spatial experiments to single parameters per map. MAPCOMP combines many input maps into one output map showing regions of similarities and dissimilarities among any number of input variables, which can be maps of model-output variables or observations or a combination of both. MAPCOMP is implemented here for the Greenland Ice Sheet and demonstrated using results from SeaRISE (Sea-level Response to Ice Sheet Evolution). Applied as a model comparison tool, results from MAPCOMP allow to determine regions where results from different models diverge. Applied in model-data comparison, MAPCOMP results indicate regions where differences to observations prevail and thus point at physical processes that need to be addressed to reduce model uncertainties across the participating models. Application to results from different experiments and scenarios, including one or several models, will aid in visual as well as quantitative assessment of probable versus less likely projected changes in calculated climatic and cryospheric variables. In general, spatial map comparison can be used as an aid to better understand model functionality, to reduce uncertainties, especially in critical regions, and to assist in assessment of future cryospheric change and sea-level rise. In the case studies presented here, the map-comparison analysis of the SeaRISE experiments also reveals several interesting applied results on the glacial change in Greenland.

1 Introduction

The multitude of physical processes that contribute to sea-level change necessitates in-depth studies that are summarized periodically in the Assessment Reports of the Intergovernmental Panel on Climate Change (IPCC) (Warrick and Oerlemans, 1990; Pachauri and Reisinger, 2007; Solomon et al., 2007; Stocker et al., 2013) and new observations, as well as recent improvements in physical models, facilitate a more accurate assessment. Prediction of contribution to sea-level rise through mass loss from the Earth's large ice sheets is largely performed by ice-dynamic models, which can be run as stand-alone models or integrated into Earth system models.

Global Circulation Models (GCMs) have been developed for a number of decades, first including Atmosphere-GCMs (AGCMs) and then Atmosphere-Ocean GCMs (AOGCMs). Several years ago, the modeling community decided to move to the next step of complexity, Earth System Models, which require coupling of numerical models that were developed for several components of the Earth System. The fact that several models have been in existence for subsystems or the Earth system motivated Model Intercomparison projects (MIPs), first in 1992 (Gates, 1992). Recently, CMIP6 (Coupled Model Intercomparison Project 6) was launched, which for the first time includes a land-ice component, the Ice Sheet Model Intercomparison Project for CMIP-6 (ISMIP6) (Nowicki et al., 2016), and a sea-ice component, the Sea-Ice Model Intercomparison Project (SIMIP) (Notz et al., 2016).

Numerical simulations resultant from ISMIP6, SIMIP and other CMIP6 projects will produce many different spatial variables, from a number of models, a number of experiments and for several scenarios. The typical approaches for analysis of multi-variate multi-model spatial experiment results, or maps, used to date (see the publications from SeaRISE and ice2sea, e.g. Bindschadler et al. (2013); Nowicki et al. (2013a, b); Gillet-Chaulet et al. (2012); Levermann et al. (2014)) are difference maps or visual comparison based on a pair of the resultant maps or alternatively plots of a summarizing parameter (one value

per map) if several maps are involved in a comparison. To provide a tool for synoptic analysis that avoids first reducing the wealth of information from several spatial experiments to single parameters per map, we introduce a spatial map comparison tool, MAPCOMP, that will facilitate spatial analysis of results from multi-variate multi-model experiments for any number of model variables and is specifically designed to match the goals and geographic regions of ISMIP6 and SIMIP, the Greenland and Antarctic Ice Sheets, the Arctic Ocean, the Circum-Antarctic Ocean and other study regions. The map comparison tool will combine many input maps into one output map showing regions of similarities and dissimilarities among any number of input variables, which can be maps of model-output variables or observations or a combination of both.

1.1 Background: CMIP6, ISMIP6 and Other MIPs

ISMIP6 is an international community effort that derives its objectives from two ideas: (a) Model-sensitivity experiments aimed at assessing the future of ice-sheet change and contribution to sea-level through mass loss from the Greenland and Antarctic Ice sheets, as investigated by SeaRISE (Sea-level Response to Ice Sheet Evolution), a US-led community organized effort to estimate the upper bound of ice-sheet contributions to sea level in the next centuries (http://websrv.cs.umt.edu/isis/index.php/SeaRISEAssessment) (Bindschadler et al., 2013; Nowicki et al., 2013a, b) and *ice2sea*, a science program funded by the European Union Framework-7 scheme to improve projections of the contribution of ice to future sea-level rise from glacier and ice-sheet models and improved data sets (http://www.ice2sea.eu/) (e.g. (Pattyn et al., 2013)), and (b) Model-Intercomparison Projects (MIPs), now under the framework of CMIP6, the Coupled Model Intercomparison Project 6 (Eyring et al., 2015). MIPs used to include Global Circulation Models (GCMs), at first Atmosphere-GCMs (AGCMs) and then Atmosphere-Ocean GCMs (AOGCMs). With ISMIP6 ice-dynamic models are for the first time participating in the Coupled Model Intercomparison Project - phase 6 (CMIP6). SeaRISE used stand-alone dynamic ice sheet models and was not designed as a model-comparison effort, but as a set of sensitivity studies. ISMIP6 is the primary activity for analysis of the Greenland and Antarctic Ice Sheets within CMIP6. The role of ISMIP6 within CMIP6, its objectives and approaches, experimental design and evaluation and analysis plan are described in Nowicki et al. (2016). The goals of ISMIP6 are (1) to assess the effect of including dynamic ice sheets in climate model and (2) to improve confidence in projections of sea level rise associated with mass loss from the Greenland and Antarctic ice sheets. ISMIP6 will utilize (standalone) ice sheet models and coupled ice-sheet — climate models. It is aimed at model comparison but also at learning about the challenges and solutions associated with coupling dynamic ice sheet models to AGCMs and AOGCMs, both of which have participated in CMIP efforts in previous phases. ISMIP6 will start with initMIP, aimed at investigating initialization-related questions and evaluating the simulated present-day state. Other ice-sheet relevant MIP projects are glacierMIP (Glacier Model Intercomparison Project) and MISOMIP (Marine Ice Sheet-Ocean Model Intercomparison Project), which targets specifically ice-ocean interaction.

The importance of data sets is illustrated by the results of (Herzfeld et al., 2012), who show that the integration of bed topography for only four major outlet glacier systems has a similar effect on the prediction of volume loss from the Greenland ice sheet, and hence on sea-level rise, as the experiment of doubled sliding for the entire Greenland ice sheet. Algebraic map comparison, also termed similarity mapping, provides a means for model-data comparison and evaluation as well.

1.2 Need for a Diagnostic Tool for Spatial Analysis of Multi-Model Multi-Experiment Multi-Variable and Multi-Data Set Results

The planned experiments for ISMIP6 are described in Nowicki et al. (2016). In summary, many different model variables will be output, resultant from many different participating models, under many different scenarios and experiments. To learn from these, as is the goals of ISMIP6 and CMIP6, analysis and evaluation tools are required. The main deficiency shared by all previously used diagnostic tools is that the spatial information resultant from the experiments is reduced before it is analyzed. The typical approaches used to date for comparative analysis of multi-variate multi-variate spatial experiments fall into two classes: The first type of comparisons uses a summarizing parameter for each map, such as average elevation change or volume loss for an entire region, as illustrated in examples from Nowicki et al. (2013a) and Bindschadler et al. (2013) (Figures 1-3). The second type uses pairwise comparisons of two model outputs, or maps, typically an experiment result minus a control run for one model at a time, examples are found in Nowicki et al. (2013a, b), or visual comparison between a model run and a data set. Analysis of large ensembles, where the variability is reduced to the mean of all participating models (e.g. Kay et al. (2011)), are another example of data reduction before analysis, which hides the contributions of individual models or regions (depending on whether maps or summarizing graphs are plotted). The map comparison method does not require an information reduction prior to spatial analysis and allows to investigate spatial relationships among any number of maps or models; this is afforded by use of an algebraic semi-norm in a space whose order is the number of possible comparisons.

A web-based tool designed to aid in model-data comparison by facilitating searches for altimeter data from ICESat's Geoscience Laser Altimeter System (GLAS) (Schutz et al., 2005; Zwally et al., 2005) and gravity data from the Gravity Recovery and Climate Experiment (GRACE) in the neighborhood of any point in a modeling grid is under development and described in Price et al. (2016 in press). The idea of this tool is to enable comparison between a given, single model and observations from a satellite mission locally or regionally. While the tool by Price et al. (2016 in press) offers web-based access, its quantitative metrics are limited to a number of summative statistical calculations and evaluation of one model with one data set at a time. The MAPCOMP similarity mapping approach described here allows diagnostics of any number of models, experiments and data sets synoptically, which may include time series of ice-sheet-wide grid models from altimetry, gravity, bed topography or other satellite, airborne or field campaigns. In that they include different forms of flexibility, the two approaches may be considered complimentary.

1.3 Objectives

The objective of this paper is to demonstrate the capabilities of the MAPCOMP method for model evaluation, model-data comparison, and comparative regional analysis of experiment results. Experiments from SeaRISE will be analyzed to illustrate the map comparison approach, since those results are already available to the community at large. The expected results from the several planned phases of ISMIP-6, starting with initMIP, will use the same data formats and variables as SeaRISE (http://websrv.cs.umt.edu/isis/index.php/SeaRISEAssessment).

2 Approach: The Algebraic Map Comparison Method

2.1 Overview

Algebraic similarity mapping utilizes the algebraic map comparison method first derived in Herzfeld and Merriam (1990) as an aid in petroleum exploration based on several geophysical and geologic maps. Applications in exploration geology, basin analysis, oceanography and marine geology are reported in Merriam et al. (1993a, b); Hamann and Herzfeld (1991); Herzfeld (1992); Merriam et al. (1999). Other methods of thematic map comparison are summarized in (Merriam and Jewett, 1988), however, the result of comparing two maps is usually a number; except for the case of a correlation map derived from two series of maps (Brower and Merriam, 1990). An application of algebraic map comparison in physical modeling is described in Herzfeld (1992).

In summary, the map-comparison algorithm utilizes a pointwise operator (the MAPCOMP-operator), which calculates a combination of distances among standardized values in pairwise comparisons of any number of input maps. In simplified terms, one may envision that the MAPCOMP-operator moves across the study area and derives a similarity value at each (grid) location from a stack of maps. An input map can be a gridded data set for the study area, or the result of a numerical model run.

Mathematically, similarity mapping is based on an algebraic approach that proceeds by (1) standardizing input values in each map or spatial model, (2) forming a functional of pairwise differences of standardized values, and (3) applying a semi-norm to the functional in (2), which results in a similarity value $F(x)$ in each point x in a map area M. The result is a spatial grid model of similarity values, which may be contoured, displayed as a 3-dimensional model, or utilized as an input layer in a geographical information system (GIS) or in a physical model. The next sections detail the mathematical principles as well as options for handling missing data values and integrating boundaries of geographic areas.

Standardization is necessary, wherever data from different sources or variables of different units are to be analyzed synoptically. Here, we use linear transformation of the range of data into the interval [0,1] or a log-linear transformation. Similarity values close to 0 indicate good similarity, while higher values indicate poor correspondence among the input maps or models in a given location. The largest similarity value is 1.

In the experiments in this paper, the region is Greenland, but as the ice sheet retreats, the region of comparison changes specifically for some models. This problem can be addressed using the G and F comparison options described below.

2.2 Standardization

Comparison of different variables requires pre-analysis standardization. In this paper, the proportion-of-range standardization is applied, which is defined as follows:

Definition. Proportion-of-range standardization. If $ymin_j$ and $ymax_j$ are the minimal and maximal values observed on the variable y_j (for $j = 1, \ldots, n$ with n the number of variables, e.g. velocity, surface elevation, basal water, measured or modeled),

and y_{ij} are observations of y_j (for $i = 1, \ldots, r_j$, r_j the number of observations/ model values on y_j), then the proportion-of-range standardization z_p is defined by

$$z_p(y_{ij}) = \frac{y_{ij} - ymin_j}{ymax_j - ymin_j} \tag{1}$$

We may also write $\overline{y} = z_p(y)$ for a standardized value. If one variable generally increases where most others decrease, then inverse proportion-of-range standardization z_{p^-} is used:

$$z_{p^-}(y_{ij}) = \frac{ymax_j - y_{ij}}{ymax_j - ymin_j} \tag{2}$$

Note that $z_{p^-}(y_{ij}) = 1 - z_p(y_{ij})$. Both proportion-of-range standardizations map the observed data range into the interval [0,1]. The proportion-of-range transformation considers all data values equally important and is associated with the uniform distribution. The actual distribution of a variable depends on the selection of the study area and is usually unknown or very complex for spatial environmental variables or climate variables in topographically complex areas. In such cases, assumption of a uniform rather than a Gaussian distribution commonly leads to more robust results in the analysis (Hamann and Herzfeld, 1991). In consequence we utilize the proportion-of-range transformation in the application of similarity mapping to SEaRISE experiment results.

Log-linear transformation. Because the velocities of the fast-moving outlet glaciers are higher than the flow velocities of the inland ice sheets by orders of magnitude, a logarithmic transformation of velocity is not only a better means of visualization, but also provides a more balanced input in the map comparison. This motivates application of a log-linear transformation.

Definition. Log-linear transformation. Using notation as above and

$$z_{ln}(y_{ij}) = ln(y_{ij}) \tag{3}$$

for the natural logarithmic transformation, we introduce the notation

$$z_{ln,p}(y_{ij}) = z_p(z_{ln}(y_{ij})) \tag{4}$$

for the log-linear transformation. Note that the variable values are first transformed logarithmically and then proportion-or-range standardization is applied.

Figures 1 and 2 illustrate the differences of the proportion-of-range standardization and the log-linear transformation. For Figure 1 velocities from four models are standardized uniformly (using proportion-of-range standardization), then run through MAPCOMP, which yields a resultant similarity map with values in the interval [0,1]. However, since velocities differ by orders of magnitude between the interior of the ice sheet and the fast-moving outlet glaciers, the similarity map shows high similarity throughout much of the study region, as seen in the middle panel of Figure 1. The regional differences in the similarity map are best visualized using a logarithmic transformation into the range of exponent -9 (similarity value close to zero) to 0 ($e^0 = 1$), i.e. a logarithmic color scale, as shown in the lowest panel of Figure 1. Alternatively, the values of the velocity magnitudes

from four models are first transformed logarithmically, then standardized uniformly, then run through MAPCOMP, and results plotted with a linear color scale, as shown in Figure 2. In most of the analyses in this paper we will utilize the log-linear transformation for velocity magnitudes and the linear proportion-of-range standardization (uniform) standardization for other variables.

2.3 The MAPCOMP Algorithm

The algebraic map comparison algorithm is based on the calculation of weighted averages beween standardized values of any pair of input maps, for each point of the map area (in practice, for each node of a common underlying grid). Let M denote a map area, n the number of input maps and $M_1, \ldots, M_n$ the input maps with $\overline{m_k(x)}$ the standardized value of map M_k at location x. For each grid point $x \in M$ a difference matrix $D(x) \in \mathcal{R}^{n,n}$ is formed with elements $d_{st}(x) = \overline{m_s(x)} - \overline{m_t(x)}$, note that different types of standardization may be used in each map, $M_s, M_t, s, t = 1, \ldots, n$. As x varies over the study area, $D(x)$ becomes a matrix functional. Now we define a norm in $\mathcal{R}^{n,n}$ as

$$F(x) = \frac{1}{k} \sum_{s<t,\ t=1}^{n} |d_{st}(x)| \tag{5}$$

with $k = n(n-1)/2$, the number of different pairwise comparisons among the n maps. $F(x)$ represents the average difference between maps at location x, hence $F(x)$ is low if the maps are similar and high if they are different.

Use of equation (3) assumes that all input maps are of equal importance. In a practical situation, however, one can imagine that one map may be considered more important, or that a model is to be compared with several different input maps. It may also be the case that a change in one variable has more drastic consequences for the environment than a change in another variable, for instance, imagine a 50% increase in wind speed versus a 50% increase in precipitation.

To meet similar requirements, we assign a weight w_i to the input map M_i for each $i \in 1, \ldots, n$ that captures the importance of map M_i. (Note that all weights must be nonnegative and at least one positive). The MAPCOMP equation for F including weighted input maps is given by

$$F(x) = \frac{\sum_{s<t,\ t=1}^{n} w_s w_t |\overline{m_s(x)} - \overline{m_t(x)}|}{\sum_{s<t,\ t=1}^{n} w_s w_t} \tag{6}$$

If a zero weight is used, the right-hand-side of equation (5) is actually only a semi-norm.

Calculating $F(x)$ over the whole study area, i.e. for every location $x \in M$, we build a grid model for the similarity map F. This grid model may be visualized as a map which shows relative values, giving the quality of agreement of the input maps. If a proportion-of-range standardization is used, then the values in the similarity map will also lie between 0 and 1, with low values indicating good correspondence among the input maps in a given location, and higher values indicating poor similarity. As a rule of thumb, a value below 0.2 indicates good similarity in comparisons with nine or more maps, and a value above 0.5 indicates very poor similarity.

In equations (3) and (4), the 1-norm (absolute value) is employed to form $d_{st}(x)$, i.e. the absolute value of pairwise differences of map values. One may also base the MAPCOMP equation on other norms, such as the Euclidean norm (2-norm) or the Mahalanobis norm. We have chosen the 1-norm for reasons of robustness in the ensuing data analysis.

A resultant value on the comparison map F can stem from the fact that all maps are slightly different, or the fact that all but one are similar and one map differs from all the others. In that situation, a visual test may help to find the outlier. Using the MAPCOMP program, it is easy to compare only some of the n maps by setting some weights to zero, and thus determine significant connections (Herzfeld and Sondergard 1988).

2.4 Missing-Data Handling and Working with Land Masks (e.g. Greenland)

Data may be missing at some of the grid nodes in the map area M, and this could happen at different locations of the individual maps. The program MAPCOMP offers two possibilities to handle such situations:

(i) F-algorithm: At location $x \in M$, only the maps that have data at x are compared.

(ii) G-algorithm: At location $x \in M$, the comparison value is only calculated if all n maps have values at location x.

In subareas where all maps have data, F and G coincide. If only one map has a value at a point x, no comparison is done. In places where 2 to $(n-1)$ maps have data, an F-map may be obtained, but not a G-map. The advantage of the F-map algorithm is that comparison is carried through in a larger part of the area. On the other hand, G maps are easier to read, since all map areas are supported by the same number of input data fields. In the examples, the F algorithm was applied.

In our analysis of results from the SeaRISE project, the region is not a rectangle. MAPCOMP, implemented for Greenland, takes care of those requirements. A land-mask file can be created that is a matrix of a rectangular envelope of the study area in the projection that is to be used in the similarity mapping. Indicator values are used to identify grid nodes inside the study area and outside the study area, notably the area need not be simply connected but may have any shape. In combination with the F and G-algorithm options for missing data values, many different situations of data coverage can now be incorporated in a synoptic study.

2.5 Data Format

SeaRISE model results are stored in netCDF format and follow the Climate and Forecast metadata conventions. Results for Greenland are given in Polar Stereographic coordinates on a standard 5 km grid of 301 $\times$ 561 points. Model experiments begin on 2004-01-01 and are run forward 500 years storing the output variables every 5 years. One netCDF file is given per model per experiment. These files are easily read by common scientific software, such as MATLAB or python, where each variable in a given file can be loaded as a 3-dimensional array (x-y-time). MAPCOMP takes as input any 2-dimensional array (or map) on a standard grid and can therefore use any combination of model output at any time index.

One of the standard outputs for SeaRISE data are masks for ocean, land, ice and for some models, ice-shelves. To make sensible comparisons, we apply the respective ice masks to each of the 2D data arrays we wish to compare to attain only information about the ice-sheet. Locations outside the ice-mask are given not-a-number (NaN) values which are ignored by

the algorithm. Additionally, the land mask is used for plotting purposes while the ice-shelf mask is not used for any of the examples given in this paper.

3 SeaRISE Experiments and Participating Models

3.1 Experiments

The SeaRISE experiments are described in (Bindschadler et al., 2013; Nowicki et al., 2013a, b). Briefly, those are

(CC) Control run, using constant climate for the new 500 years

(C1) Temperature and precipitation set to the A1B forcings

(C2) Temperature and precipitation set to the 1.5 times the A1B forcings

(C3) Temperature and precipitation set to the 2 times the A1B forcings

(S1) Doubled basal sliding velocities for the entire Greenland ice sheet, including all outlet glaciers

(S2) 2.5 times basal sliding velocities for the entire Greenland ice sheet, including all outlet glaciers

(S3) 3 times basal sliding velocities for the entire Greenland ice sheet, including all outlet glaciers

(M1) Prescribed basal melt rates of 2 m/yr at the ice-ocean boundaries around Greenland

(M2) Prescribed basal melt rates of 20 m/yr at the ice-ocean boundaries around Greenland

(M3) Prescribed basal melt rates of 200 m/yr at the ice-ocean boundaries around Greenland

(C1S1) Combination of C1 and S1 (also labeled T1)

(R8) More realistic scenario for IPCC AR5, R8 (also labeled FF)

The SeaRISE experiments include several groups: Atmospheric experiments (C1, C2, C3) are based on AR-4 temperature and precipitation change scenarios (called A1B), which prescribe a 3.5°C temperature increase over 94 years, and temperatures are held constant after that. Basal sliding experiments (S1, S2, S3) assumed an increase of sliding velocities for the entire Greenland ice sheet and could be implemented by all models. To examine the sensitivity of ice volume loss to melting at the ice-ocean flux gates, melt experiments (M1, M2, M3) were conducted using prescribed submarine melt rate anomalies, however implementation varied a lot across the participating models, because the models handle mass flux and ice-ocean boundaries in different ways. In the combination experiment C1S1 (also named T1), the conditions for S1 and C1 were both prescribed. Since all of the above experiments assume a rather drastic change from the present conditions, SeaRISE experiment R8 (also named FF) was designed to resemble a more realistic scenario (Bindschadler et al., 2013). Experiment R8 approximates one

of the so-called representative concentration pathways (RCPs) that were investigated for the 5th Assessment Report (AR5) of the Intergovernmental Panel on Climate Change (IPCC) (Meinshausen et al., 2011; Van Vuuren et al., 2011; Stocker et al., 2013). The RCPs were designed to represent possible evolutions of global human activity that provide the standard scenarios for global climate models to facilitate model comparison. However, the RCPs are provided in radiative forcing units, while the ice-sheet models require conditions for surface climate, basal sliding and ice-shelf melting forces. SeaRISE experiment R8 is built on the RCP R8.5 in this sense, as graphed and described in Bindschadler et al. (2013). Following an initialization procedure, which included a spin-up or an application of data constraints, all experiments were run forward for the next 500 years, with present being 2004. In our analyses, we use the control run (CC) and experiments C1, S1, M1, C1S1 (=T1) and R8 (=F).

3.2 Models

The models that participated in SeaRISE for Greenland are described in Wang et al. (2012); Price et al. (2011); Lemieux et al. (2011); Bougamont et al. (2011); Evans et al. (2012); Saito and Abe-Ouchi (2004, 2005, 2010); Greve et al. (2011); Morlighem et al. (2010); Seroussi et al. (2011); Larour et al. (2012); Bueler and Brown (2009); Aschwanden et al. (2011); Greve et al. (2011); Seddik et al. (2012); Greve and Herzfeld (2013); Fastook (1993); Gagliardini et al. (2013) and summarized in Nowicki et al. (2013a) (Table 1). An overview of models, model labels used in SeaRISE result data and references is given in Table 1.

4 MAPCOMP Analyses

Here we illustrate some of the possibilities for applications of MAPCOMP in comparisons across models, across variables and combinations thereof as well as model-data comparisons.

4.1 Comparison Across Models

In the first experiment, we compare results from n different numerical models for one experiment (M1) and for one geophysical variable, illustrated here for velocity magnitude, as calculated after 500-year model runs. In this analysis experiment, for each map, the velocity magnitude was standardized linearly into the range of maximum and minimum velocity of that map. In the figure panels, logarithmic scaling of the standardized values is used. Map comparison is applied unweighted and resultant values in [0,1]. Modeled velocities after experiment M1 (500 years) agree most along the ice divides, as should be expected, because all models use the same ice-surface topography (Figures 1, 2). Largest velocity differences among the 4 maps exist for fast-moving outlet glaciers: Difference values with a log of -4.5 outline the regions of fast flow of major outlet glaciers around the margin of the Greenland ice sheet. Notably, highest dissimilarity values are reached for the lower regions of (a) glaciers in central Western Greenland (Jakobshavn Isbræ, Storstrømmen and other glaciers around the Nussuaq Peninsula), and (b) glaciers in southeastern Greenland (Helheim Glacier). These glaciers fall into only two flow regions of the ice sheet. Higher similarities exist for glacier in all other regions: NW Greenland sector (Rink, Sverdrup and neighboring glaciers), northern Greenland (Humboldt, Peterman and neighboring glaciers), East Greenland (Kangerdlussuaq), and Northeastern Greenland

Table 1. SeaRISE Models

Model name	SeaRISE model abbreviation	Developers	References
Anisotropic Ice Flow Model (AIF)	WWA1, WWA2	Wei Li Wang	[Wang et al., 2012]
Community Ice Sheet Model version 2 (CISM2)	CSM2	Stephen Price, William Lipscomb	[Price et al., 2011, Lemieux et al., 2011, Bougamont et al., 2011, Evans et al., 2012]
Elmer/Ice	HSE1	Hakime Seddik	[Seddik et al., 2012]
Ice sheet model for Integrated Earth-System Studies (IcIES)	AAB1, AAB2	Ayako Abe-Ouchi, Fuyuki Saito	[Saito and Abe-Ouchi, 2004, Saito and Abe-Ouchi, 2005, Saito and Abe-Ouchi, 2010, Greve et al., 2011]
Ice Sheet System Model (ISSM)	JPL2	Eric Larour, Mathieu Morlighem, Helene Seroussi	[Morlighem et al., 2010, Seroussi et al., 2011, Larour et al., 2012]
Parallel Ice Sheet Model (PISM)	UAF1	Ed Bueler, Andy Aschwanden, Constantine Khroulev	[Bueler and Brown, 2009, Aschwanden et al., 2011]
Simulation Code for POLythermal Ice Sheet (SICOPLIS)	RGR4	Ralf Greve	[Greve et al., 2011, Greve and Herzfeld, 2013]
University of Maine Ice Sheet Model (UMISM)	JFA1	James Fastook	[Fastook, 1993]

(North-East Greenland Ice Stream). The areas of largest differences are also areas where interaction with warm ocean water is significant (Goosse and Fichefet, 1999). RGR4 and JFA1 use the JakHelKanPet bed topography, whereas JPL2 and UAF1 use the SeaRISE default topography (by Nowicki, see data website).

4.2 Comparison Across Variables

In the second experiment, the regional effect of different variables is examined for a single model (SICOPOLIS): elevation change over 500 years (ΔH), logarithmic velocity magnitude, and surface mass balance (SMB). All three variables are transformed uniformly. Results are examined for experiment C1 (temperature and precipitation change). The resultant similarity map (Figure 3) shows that the region of Humboldt Glacier has the highest values, because velocities are high, but predicted elevation changes are low and SMB is low in Northern Greenland. A second region where high dissimilarity values stand out is southeastern Greenland, where SMB is predicted highest, but velocities and elevation change are comparatively low. In this case study, the similarity maps provide a way to synoptically highlight glaciers that have an unusual behavior.

4.3 Comparison Across Models and Variables

Figure 4 illustrates that it is possible to compare across several models and several variables, here carried out for SeaRISE experiment R8 (FF). The largest signal now comes from the ice retreat that is different across the models. Application of the G-operator may avoid this effect, as only models that have “ice" grid nodes in a given location will be compared.

4.4 Model-Data Comparison and Application of Weight Factors

In the next experiment, results from the control run (CC) for six models are compared to the data set for ice-surface elevation derived by Bamber et al. (2001a). This similarity map is a way to examine the models’ ability to reproduce initial surface elevation. In Figure 5a, all models and the ice-surface elevation DEM were weighted equally (1,1,1,1,1,1,1), whereas in Figure 5b, the data set was given the same weight as all models together (1,1,1,1,1,1,6).

4.5 Application of MAPCOMP to Investigate Combination Experiments

In analyses of the SeaRISE experiments, it has been reported that volume loss results from combination experiments, such as C1S1, can be approximated at first order by the the sum of volume loss from the simple experiments (where each condition is prescribed individually), for example, volume loss from C1S1 can be reasonably approximated by volume loss from C1 plus volume loss from S1 in 100-year experiments (cf. Bindschadler et al. (2013), where temporal evolution of ice sheet volume at the continental scale is evaluated, and Nowicki et al. (2013b), where regional results from C1S1M2 are analyzed for Antarctica). Here we apply MACOMP to investigate the quality of such an approximation with respect to spatial and temporal evolution of the Greenland ice sheet in the longer, 500-year experiments for the case of the combination experiment C1S1 versus C1 and S1 run separately. Results are shown in Figure 6. As input variables, volume change is calculated for each model as the difference ΔH of surface elevation at the end of the model run (after 500 years) and at the beginning of the model run. First (see Figure 6a), a map comparison for 12 maps (6 models and 2 experiments, C1, S1) is carried out, whereas for Figure 6b, a comparison is performed for 6 elevation-change maps. Differences across models are much smaller for the two separate experiments than for the combined experiment (T1), in which both change conditions were prescribed. The analysis suggests that the two change processes enhance each other and thus result in a much larger volume loss over 500 years, than the sum of both combined. This effect is particularly strong in regions where mass loss is already high (interior of the southeast Greenland ice sheet). The spatial pattern of similarities is also different throughout the ice sheet, further supporting that the effect of the combined experiment is not equal to the sum of the effects of the individual experiments. In conclusion, the spatial and temporal evolution of the ice sheet in a combination experiment diverges significantly from that of the sum of individual experiments over 500 years. Effects of differences in ice sheet retreat are also visible.

4.6 Application of MAPCOMP to Uncover Experiment Outliers

As the example in Figure 7 shows, MAPCOMP can also be applied to find outliers among the model results. Here we see that one of the models creates different artifacts than the other models.

5 Summary and Conclusions

In this paper, we introduce an approach for spatial evaluation of model experiments, model intercomparison and model-data comparison, specifically tailored to the objectives of CMIP6. Based on the multi-variable map comparison and similarity mapping method MAPCOMP, we derive a synthesis tool for any model intercomparison or model-data evaluation project.

The method uses an algebraic semi-norm in a space with the dimension of the number comparisons possible among a set of n input variables, which can be data sets, experiment results for different variables and from different models or any combination thereof. The output is a similarity map.

Advantages of the method are: (1) The spatial relationship of each value is preserved throughout the analysis, an essential point in all geographic analysis. (2) Any number of input maps can be compared simultaneously. (3) Several standardization methods are available to integrate different variables. (4) The results are spatial data sets and hence may be presented as similarity maps or comparison maps of the study area. (5) Missing data situations can be handled by a number of options, and landmasks can be used. (6) Application of the method is straightforward and does not require specific expertise or system components, as is the case for a geographical information system.

In preparation for ISMIP6 the approach is applied to results from the SeaRISE experiments (which utilize the same format and domain as ISMIP6). The following prototypal applications are demonstrated:

(1) Model inter comparison: When applied to results from different models (run with the same settings), results from MAPCOMP show regions where models diverge or coincide.

(2) Model-data comparison: Similarity maps derived from data sets and model results reveal regions where differences to observations exist and thus may indicate situations where physical processes may need to be re-investigated or implemented differently in some models. Hence map comparison can be used as a basis for model improvement and to identify critical regions in sensitivity studies.

(3) Comparison of experiments and scenarios for one or several models: Application to results from different experiments and scenarios, including one or several models, will aid in visual as well as quantitative assessment of probable versus less likely projected changes in calculated climatic and cryospheric variables.

SeaRISE experiments C1 (temperature and precipitation change), S1 (doubled basal sliding), the combination experiment C1S1, R8 (similar to the IPCC AR4 RCP R8.5) and M1 (ice-ocean boundary induced melting) were analyzed, along with the constant-climate control run (CC). The primary objective of the analyses in this paper is the demonstration of the analysis tool. In addition, some exemplary glaciological and climatological results follow from the analyses:

(i) Comparison of modeled velocities for the experiment M1 (intended to investigate the projected influence of warming ocean water on volume loss through melt) reveal a regional segmentation of the margin of the Greenland ice sheet into (a) areas of high dissimilarity, which are the regions of high sensitivity to melting driven by warm ocean water (central Western Greenland and Southeastern Greenland), and (b) all other regions (where lower importance of ocean-induced melt processes is indicated, or simply continuation of relatively lower ocean temperatures throughout 500 years).

(ii) Comparison across variables yields similarity maps which highlight glacier systems that have unusual behavior.

(iii) While it has been hypothesized that mass loss results of a combination experiment, such as C1S1, is approximately the same as the sum of results from the individual experiments, similarity maps show that this is not the case, as large overall and regional differences exist, indicating that the prescribed changed (C1 and S1) enhance each other in the numerical experiments.

In summary, the map comparison tool provides a new level of versatility to analysis of expected results from model inter comparison projects.

6 Code and Data Availability.

Data for the SeaRISE experiments are available on the SeaRISE website (http://websrv.cs.umt.edu/isis/index.php/SeaRISEAssessment). Results from the SeaRISE experiments are available upon request from Sophie Nowicki. A development version of MACOMP for the Greenland ice sheet is available upon request from Ute Herzfeld.

Acknowledgements.

Support for research of Ute Herzfeld and Thomas Trantow through NASA Cryospheric Sciences awards NNX11AP39G and NNX16AP71G and U.S. National Science Foundation Geography and Spatial Sciences Awards 1553133 and 1553134 (BCS 1504533), for Mattia Astarita and Samuel Bennetts through University of Colorado Undergraduate Research Opportunity Program (UROP) is gratefully acknowledged. Ralf Greve and Hakime Seddik were supported by Grants-in-Aid for Scientific Research A (Nos. 22244058, 25241005 and 16H02224) of the Japan Society for the Promotion of Science (JSPS). Ralf Greve was further supported by the Arctic Challenge for Sustainability (ArCS) project of the Japanese Ministry of Education, Culture, Sports, Science and Technology (MEXT). Byron Parizek was supported by National Aeronautics and Space Administration grant NNX15AH84G and U.S. National Science Foundation grants PLR-1443190, ANT-0424589, AGS-1338832. Thanks are due to Matthew Beckley, NASA Goddard Space Flight Center, for help with making data sets available and to Samuel Bennetts, University of Colorado Boulder, for help with paper preparation.

References

Aschwanden, A., Bueler, E., Khroulev, C., and Blatter, H.: An enthalpy formulation for glaciers and ice sheets, J. Glaciol., submitted, 2011.

Bamber, J., Layberry, R., and Gogenini, S.: A new ice thickness and bed data set for the Greenland ice sheet 1: Measurement, data reduction, and errors, J. Geophys. Res., 106 (D24), 33 773–33 780, 2001a.

Bamber, J. L., Ekholm, S., and Krabill, W. B.: A new, high-resolution digital elevation model of Greenland fully validated with airborne laser altimeter data, Journal of Geophysical Research: Solid Earth (1978–2012), 106, 6733–6745, 2001b.

Bindschadler, R., Nowicki, S., Abe-ouchi, A., Aschwanden, A., Choi, H., Fastook, J., Granzow, G., Gutowski, G., Herzfeld, U., Jackson, C., Johnson, J., Khroulev, C., Levermann, A., Lipscomb, W. H., Martin, M. A., Morlighem, M., Parizek, B., Pollard, D., PRICE, S., Ren, D., Saito, F., Sato, T., Seddik, H., Seroussi, H., Takahashi, K., Walker, R., and Wang, W. L.: Ice-Sheet Model Sensitivities to Environmental Forcing and Their Use in Projecting Future Sea-Level (The SeaRISE Project), Journal of Glaciology, 59, doi:10.3189/2013JoG12J125, 2013.

Bougamont, M., Price, S., Christoffersen, P., and Payne, A.: Dynamic patterns of ice stream flow in a 3-D higher-order ice sheet model with plastic bed and simplified hydrology, Journal of Geophysical Research: Earth Surface, 116, 2011.

Brower, J. and Merriam, D.: Geological map analysis and comparison by several multivariate algorithms, Statistical applications in the earth sciences: Geol. Survey Canada Paper, pp. 89–9, 1990.

Bueler, E. and Brown, J.: The Shallow shelf approximation as a sliding law in a thermomechanically coupled ice sheet model, J. Geophys. Res., 114, 1–21, doi:10.1029/2008JF001179, http://www.agu.org/pubs/crossref/2009/2008JF001179.shtml, 2009.

Evans, K. J., Salinger, A. G., Worley, P. H., Price, S. F., Lipscomb, W. H., Nichols, J. A., White, J. B., Perego, M., Vertenstein, M., Edwards, J., et al.: A modern solver interface to manage solution algorithms in the Community Earth System Model, International Journal of High Performance Computing Applications, 26, 54–62, 2012.

Eyring, V., Bony, S., Meehl, G., Senior, C., Stevens, B., Stouffer, R., and Taylor, K.: Overview of the Coupled Model Intercomparison Project Phase 6 (CMIP6) experimental design and organisation, Geoscientific Model Development, 2015.

Fastook, J. L.: The finite-element method for solving conservation equations in glaciology, Computational Science and Engineering, 1, 55–67, 1993.

Gagliardini, O., Zwinger, T., Gillet-Chaulet, F., Durand, G., Favier, L., Fleurian, B. d., Greve, R., Malinen, M., Martín, C., and Råback, P.: Capabilities and performance of Elmer/Ice, a new generation ice-sheet model, Geoscientific Model Development Discussions, 6, 1689–1741, 2013.

Gates, W. L.: AMIP: The atmospheric model intercomparison project, Bulletin of the American Meteorological Society, 73, 1962–1970, 1992.

Gillet-Chaulet, F., Gagliardini, O., Seddik, H., Nodet, M., Durand, G., and Ritz, C.: Greenland ice sheet contribution to sea-level rise from a new-generation ice-sheet model, The Cryosphere, 6, 1561–1576, 2012.

Goosse, H. and Fichefet, T.: Importance of ice-ocean interactions for the global ocean circulation: A model study, Journal of Geophysical Research: Oceans, 104, 23 337–23 355, 1999.

Greve, R. and Herzfeld, U.: Resolution of ice streams and outlet glaciers in large-scale simulations of the Greenland ice sheet, Annals of Glaciology, 54(63), 209–220, doi:10/3189/2013AoG63A085, 2013.

Greve, R., Saito, F., and Abe-Ouchi, A.: Initial results of the SeaRISE numerical experiments with the models SICOPOLIS and IcIES for the Greenland ice sheet, Annals of Glaciology, 52, 23–30, 2011.

Hamann, I. and Herzfeld, U.: On the effects of pre-analysis standardization, J. Geology, 99, 621–631, 1991.

Herzfeld, U.: Quantitative spatial models of Atlantic primary productivity:An application of geomathematics, J. Geophys. Research Oceans, 97, 717–732, 1992.

Herzfeld, U., Fastook, J., Greve, R., McDonald, B., Wallin, B., and Chen, P.: On the influence of Greenland outlet glacier bed topography on results from dynamic ice sheet models, Annals of Glaciology, 53, 281–293, doi:10.3189/2012AoG60A061, 2012.

Herzfeld, U. C. and Merriam, D. F.: A map comparison technique utilizing weighted input parameters, Computers & Geology, 7, 43–52, 1990.

Kay, J. E., Holland, M. M., and Jahn, A.: Inter-annual to multi-decadal Arctic sea ice extent trends in a warming world, Geophysical Research Letters, 38, 2011.

Larour, E. H., Seroussi, H., Morlighem, M., and Rignot, E.: Continental scale, high order, high spatial resolution, ice sheet modeling using the Ice Sheet System Model (ISSM), J. Geophys. Res, 117 (F1), F01 022, 2012.

Lemieux, J.-F., Price, S. F., Evans, K. J., Knoll, D., Salinger, A. G., Holland, D. M., and Payne, A. J.: Implementation of the Jacobian-free Newton–Krylov method for solving the first-order ice sheet momentum balance, Journal of Computational Physics, 230, 6531–6545, 2011.

Levermann, A., Winkelmann, R., Nowicki, S., Fastook, J. L., Frieler, K., Greve, R., Hellmer, H. H., Martin, M. A., Meinshausen, M., Mengel, M., Payne, A. J., Pollard, D., Sato, T., Timmermann, R., Wang, W. L., and Bindschadler, R. A.: Projecting Antarctic ice discharge using response functions from SeaRISE ice-sheet models, Earth System Dynamics, 5, 271–293, doi:10.5194/esd-5-271-2014, www.earth-syst-dynam.net/5/271/2014/, 2014.

Meinshausen, M., Smith, S. J., Calvin, K., Daniel, J. S., Kainuma, M., Lamarque, J., Matsumoto, K., Montzka, S., Raper, S., Riahi, K., et al.: The RCP greenhouse gas concentrations and their extensions from 1765 to 2300, Climatic change, 109, 213–241, 2011.

Merriam, D. and Jewett, D.: Methods of thematic map comparison, in: Current trends in geomathematics, pp. 9–18, Springer, 1988.

Merriam, D., Fuhr, B., and Herzfeld, U.: An integrated approach to basin analysis and mineral exploration, in: Computerized basin analysis, pp. 197–214, Springer, 1993a.

Merriam, D., Herzfeld, U., and A.: Integration of geophysical data for basin analysis, Brasilian Geophys. Soc., 2, 1025–1030, 1993b.

Merriam, D., Herzfeld, U., and Fuhr, B.: An integrated mapping approach to petroleum exploration on the Pratt anticline, Pratt County, Kansas, Natural Resources Research, 8, 69–86, 1999.

Morlighem, M., Rignot, E., Seroussi, H., Larour, E., Ben Dhia, H., and Aubry, D.: Spatial patterns of basal drag inferred using control methods from a full-Stokes and simpler models for Pine Island Glacier, West Antarctica, Geophysical Research Letters, 37, 2010.

Notz, D., Jahn, A., Holland, M., Hunke, E., Massonnet, F., Stroeve, J., Tremblay, B., and Vancoppenolle, M.: Sea Ice Model Intercomparison Project (SIMIP): Understanding sea ice through climate-model simulations, Geoscientific Model Development Discussions, 2016, 1–29, doi:10.5194/gmd-2016-67, http://www.geosci-model-dev-discuss.net/gmd-2016-67/, 2016.

Nowicki, S., Bindschadler, R., Abe-ouchi, A., Aschwanden, A., Choi, H., Fastook, J., Granzow, G., Gutowski, G., Herzfeld, U., Jackson, C., Johnson, J., Khroulev, C., Levermann, A., Lipscomb, W. H., Martin, M. A., Morlighem, M., Parizek, B., Pollard, D., Price, S., Ren, D., Saito, F., Sato, T., Seddik, H., Seroussi, H., Takahashi, K., Walker, R., and Wang, W. L.: Spatial sensitivities of the Greenland Ice Sheet to Environmental Changes (The SeaRISE Project), Journal of Geophysical Research - Earth Surface, pp. 1025–1044, doi:10.1002/jgrf.20076, 2013a.

Nowicki, S., Bindschadler, R., Abe-ouchi, A., Aschwanden, A., Choi, H., Fastook, J., Granzow, G., Gutowski, G., Herzfeld, U., Jackson, C., Johnson, J., Khroulev, C., Levermann, A., Lipscomb, W. H., Martin, M. A., Morlighem, M., Parizek, B., Pollard, D., Price, S., Ren, D.,

Saito, F., Sato, T., Seddik, H., Seroussi, H., Takahashi, K., Walker, R., and Wang, W. L.: Spatial sensitivities of the Antarctic Ice Sheet to Environmental Changes (The SeaRISE Project), Journal of Geophysical Research - Earth Surface, pp. 1002–1024, doi:10.1002/jgrf.20081, 2013b.

Nowicki, S. M. J., Payne, T., Larour, E., Seroussi, H., Goelzer, H., Lipscomb, W., Gregory, J., Abe-Ouchi, A., and Shepherd, A.: Ice Sheet Model Intercomparison Project (ISMIP6) contribution to CMIP6, Geoscientific Model Development Discussions, 2016, 1–42, doi:10.5194/gmd-2016-105, http://www.geosci-model-dev-discuss.net/gmd-2016-105/, 2016.

Pachauri, R. and Reisinger, A.: Climate Change 2007: Synthesis Report. Contribution of Working Groups I, II and III to the Fourth Assessment Report of the Intergovernmental Panel on Climate Change, Geneva: IPCC, 2007.

Pattyn, F., Perichon, L., Durand, G., Favier, L., Gagliardini, O., Hindmarsh, R. C., Zwinger, T., Albrecht, T., Cornford, S., Docquier, D., et al.: Grounding-line migration in plan-view marine ice-sheet models: results of the ice2sea MISMIP3d intercomparison, Journal of Glaciology, 59, 410–422, 2013.

Price, S. F., Payne, A. J., Howat, I. M., and Smith, B. E.: Committed sea-level rise for the next century from Greenland ice sheet dynamics during the past decade, Proceedings of the National Academy of Sciences, 108, 8978–8983, 2011.

Price, S. F., Hoffman, M. J., Bonin, J. A., Howat, I. M., Neumann, T., Saba, J., Tezaur, I., Guerber, J., Chambers, D. P., Evans, K. J., Kennedy, J. H., Lenaerts, J., Lipscomb, W. H., Perego, M., Salinger, A. G., Tuminaro, R. S., van den Broeke, M. R., and Nowicki, S. M. J.: An ice sheet model validation framework for the Greenland ice sheet, Geoscientific Model Development, 2016, 1–29, doi:10.5194/gmd-2016-97, http://www.geosci-model-dev-discuss.net/gmd-2016-97/, 2016 in press.

Saito, F. and Abe-Ouchi, A.: Thermal structure of Dome Fuji and east Dronning Maud Land, Antarctica, simulated by a three-dimensional ice-sheet model, Annals of Glaciology, 39, 433–438, 2004.

Saito, F. and Abe-Ouchi, A.: Sensitivity of Greenland ice sheet simulation to the numerical procedure employed for ice-sheet dynamics, Annals of Glaciology, 42, 331–336, 2005.

Saito, F. and Abe-Ouchi, A.: Modelled response of the volume and thickness of the Antarctic ice sheet to the advance of the grounded area, Annals of Glaciology, 51, 41–48, 2010.

Schutz, B., Zwally, H., Shuman, C., Hancock, D., and DiMarzio, J.: Overview of the ICESat Mission, Geophysical Research Letters, 32, doi:10.1029/2005GL024009, 2005.

Seddik, H., Greve, R., Zwinger, T., Gillet-Chaulet, F., and Gagliardini, O.: Simulations of the Greenland ice sheet 100 years into the future with the full Stokes model Elmer/Ice, Journal of Glaciology, 58, 427–440, 2012.

Seroussi, H., Morlighem, M., Rignot, E., Larour, E., Aubry, D., Ben Dhia, H., and Kristensen, S. S.: Ice flux divergence anomalies on 79north Glacier, Greenland, Geophysical Research Letters, 38, 2011.

Solomon, S., Qin, D., Manning, M., Chen, Z., Marquis, M., Avery, K., Tignor, M., and Miller, H.: Climate change 2007: The physical science basis: contribution of Working Group I to the Fourth Assessment Report of the Intergovernmental Panel on Climate Change, Cambridge University Press, 2007.

Stocker, T. F., Qin, H., Plattner, G.-K., Tignor, M., Allen, S. K., Boschung, J., Nauels, A., Xia, Y., Bex, V., and Midgley, P. M. e.: Climate Change 2013: The Physical Science Basis. Contribution of Working Group I to the Fifth Assessment Report of the Intergovernmental Panel on Climate Change, Cambridge University Press, 2013.

Van Vuuren, D. P., Edmonds, J., Kainuma, M., Riahi, K., Thomson, A., Hibbard, K., Hurtt, G. C., Kram, T., Krey, V., Lamarque, J.-F., et al.: The representative concentration pathways: an overview, Climatic change, 109, 5–31, 2011.

Wang, W., Li, J., and Zwally, H. J.: Dynamic inland propagation of thinning due to ice loss at the margins of the Greenland ice sheet, Journal of Glaciology, 58, 734–740, 2012.

Warrick, R. and Oerlemans, J.: Sea level rise, in: Climate Change - The IPCC Scientific Assessment, Cambridge University Press, 1990.

Zwally, H., Giovinetto, M., J.Li, Cornejo, H., M.Beckley, Brenner, A., Saba, J., and Yi, D.: Mass changes of the Greenland and Antarctic ice sheets and shelves and contributions to sea-level rise: 1992–2002, Journal of Glaciology, 51, 509–527, 2005.

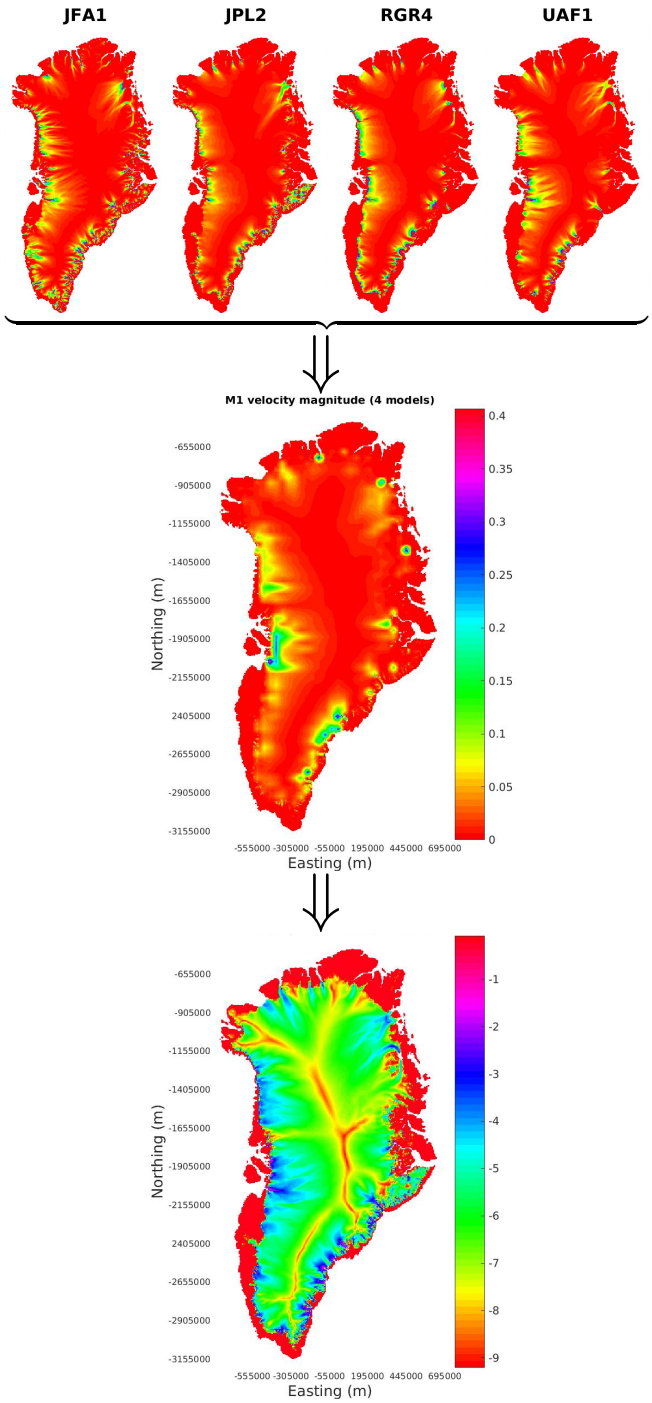

Figure 1. MAPCOMP applied to 4 models and 1 variable (velocity). Comparison of velocity magnitude from the end state of experiment M1 (after 500 years) using four models: JFA1, JPL2, RGR4 and UAF1. Modeled velocity magnitudes standardized linearly (using proportion-of-range standardization) for the 4 input maps of MAPCOMP. Resultant similarity map (shown in the middle) is best visualized using a log-linear color-scale (bottom panel).

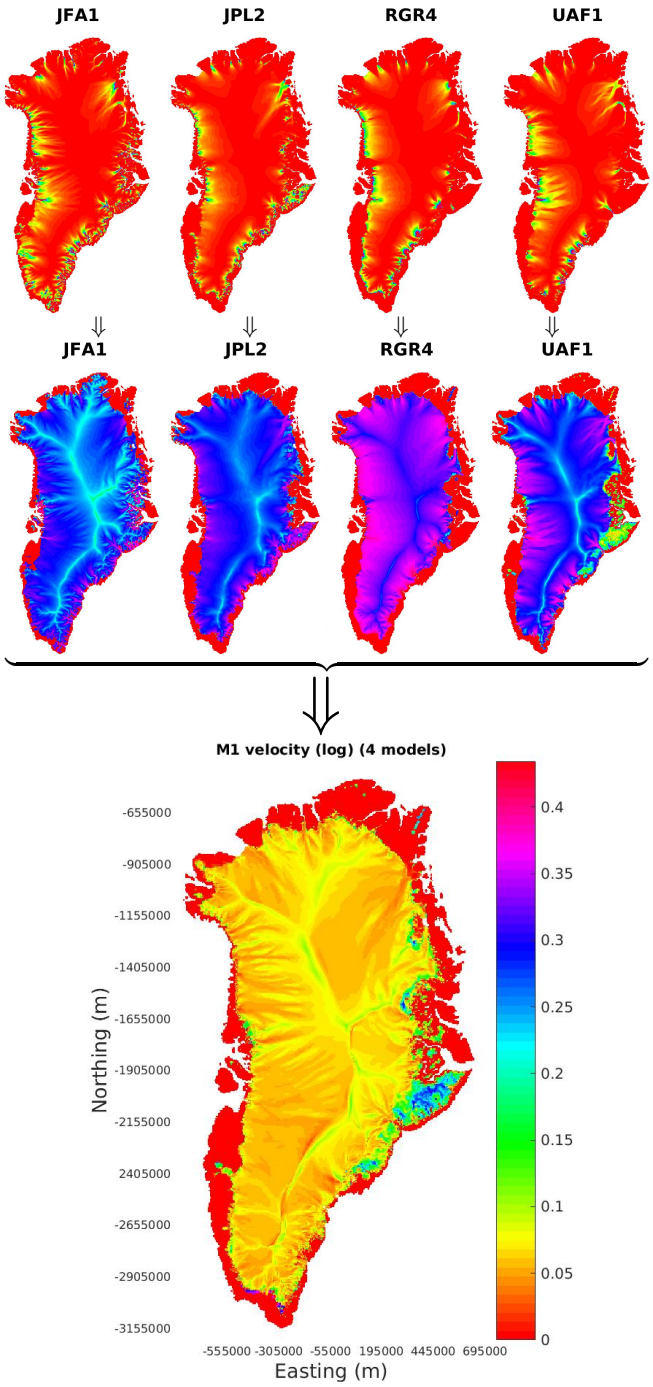

Figure 2. MAPCOMP log-linear standardization of input maps, illustrated for 4 models and 1 variable (velocity). Log-linear transformation is applied to the velocity magnitude for each input map of MAPCOMP. Resultant similarity values are in the interval [0,1]. Comparison with Figure 1 shows the effect of linear versus log-linear standardization. In the similarity map, red areas around the periphery showing perfect similarity correspond to ice-free terrain in all inputs.

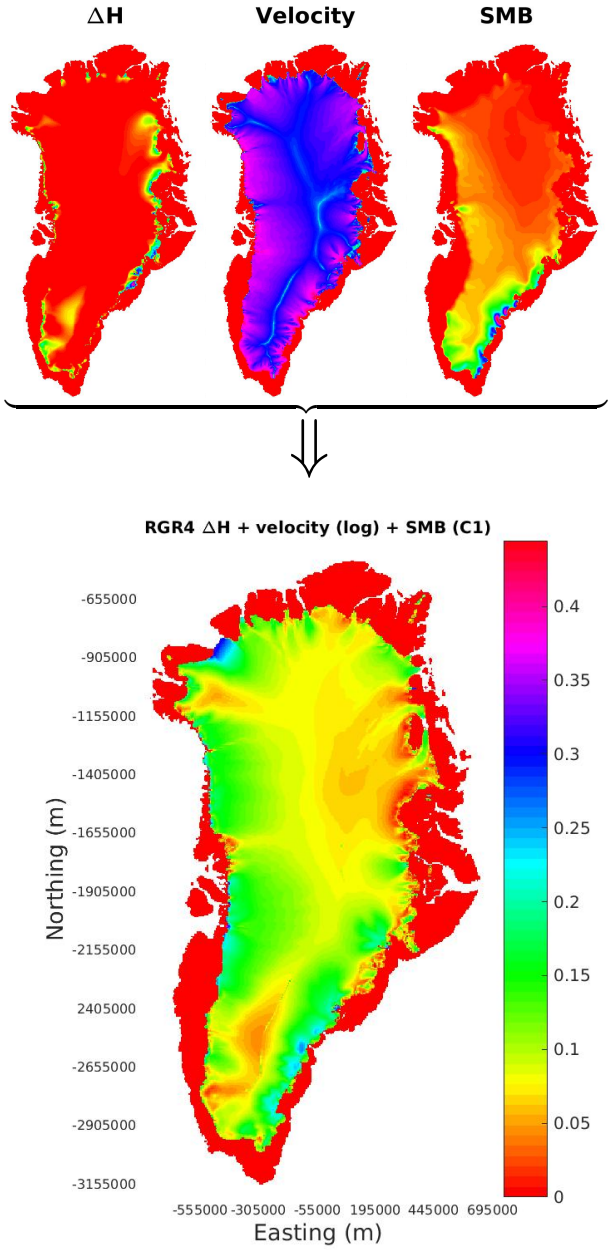

Figure 3. MAPCOMP applied to 1 model and 3 variables, using results for ice thickness (standardized linearly), velocity magnitude (log-linearly transformed) and surface mass balance (SMB, standardized linearly) from the RGR4 model in the C1 experiment. Red areas around the periphery showing perfect similarity correspond to ice-free terrain in all inputs.

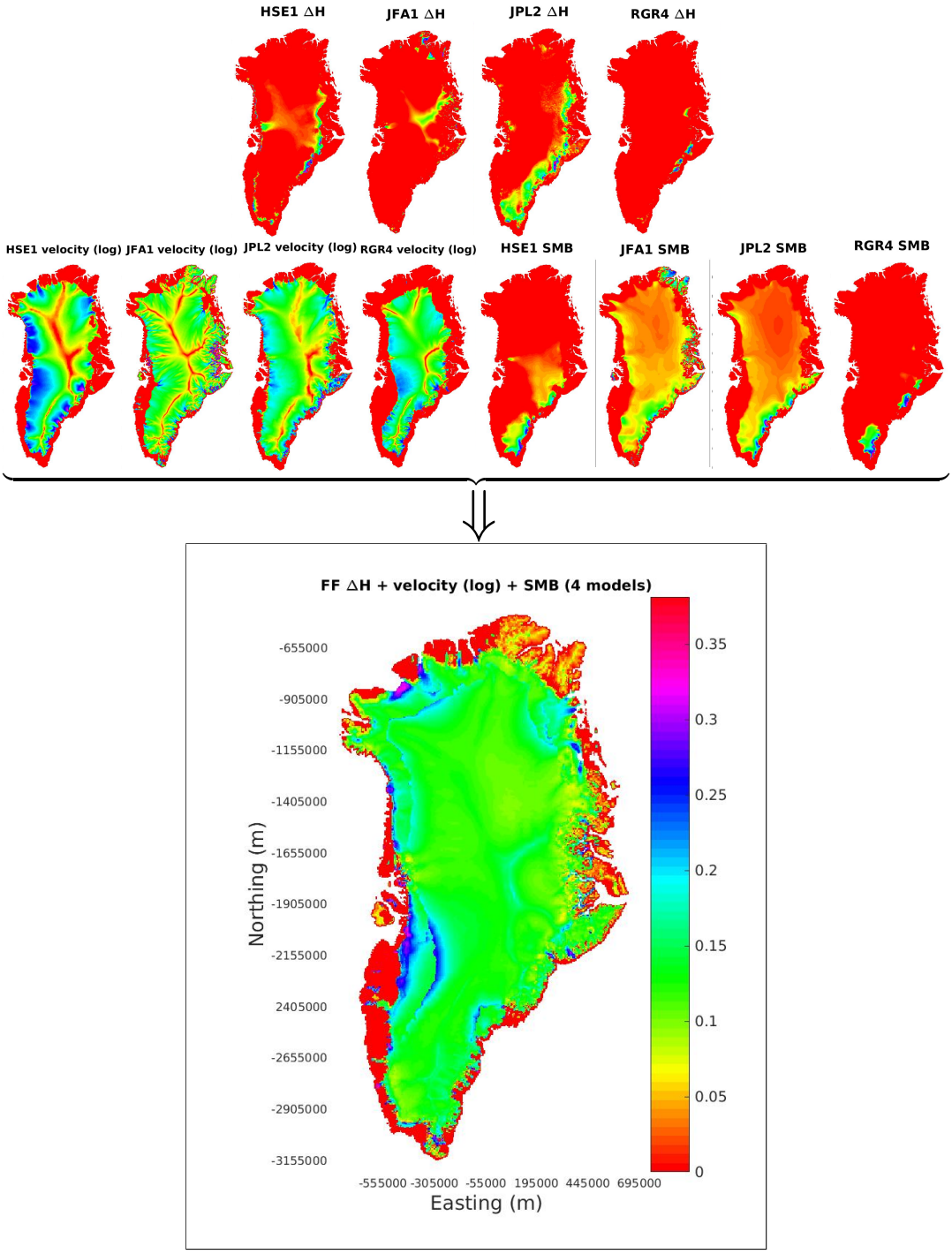

Figure 4. MAPCOMP applied to 6 models and 3 variables, using results from the R8 (FF) experiment for the JFA1, JPL2, HSE1 and RGR4 models to compare change in thickness (standardized linearly), velocity magnitude (log-linearly transformed) and surface mass balance (SMB, standardized linearly). In the similarity map, red areas around the periphery showing perfect similarity correspond to ice-free terrain in all inputs.

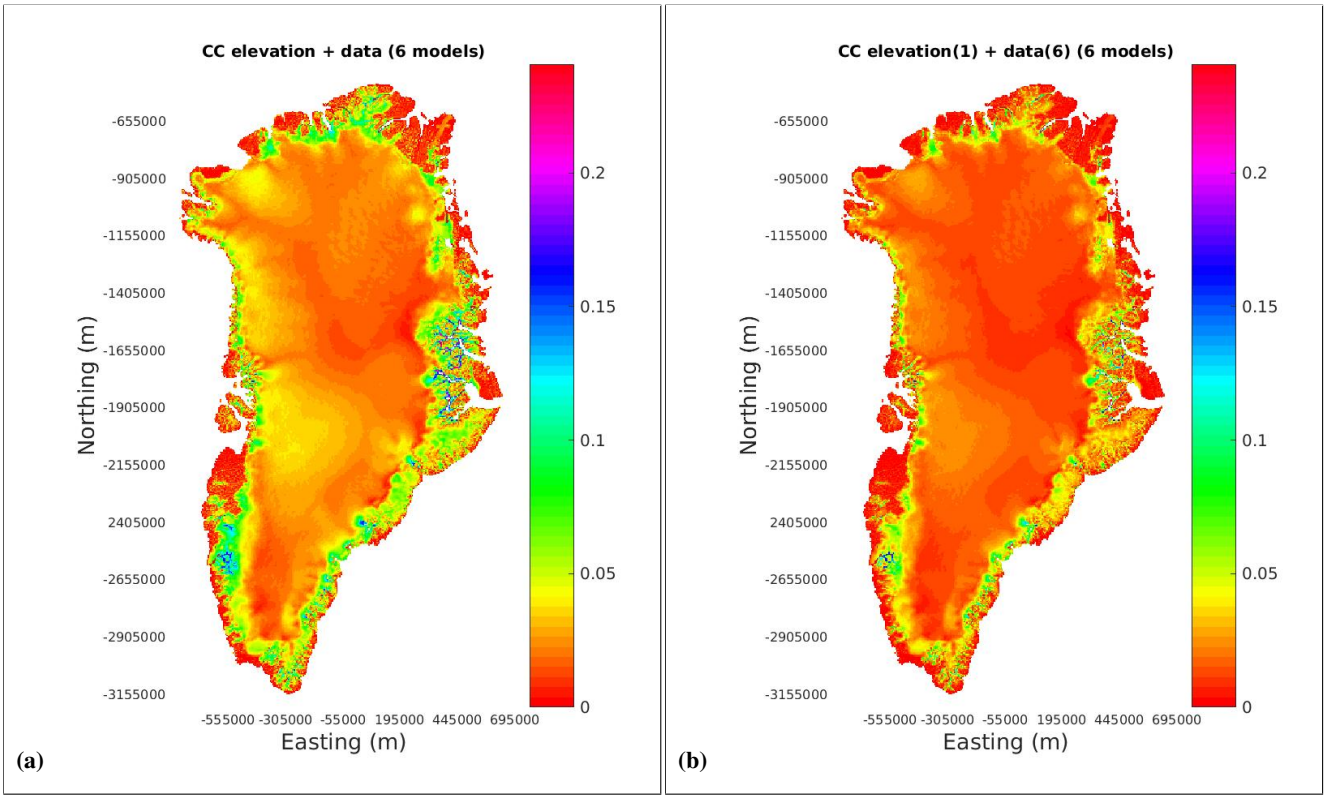

Figure 5. MACOMP comparison of models and data (a) unweighted and (b) weighted. Both maps compare the 5-km surface DEM of Bamber et al. (2001b) and the initial elevations in the CC (control) experiment for the CSM2, JFA1, JPL2, HSE1, UAF1 and RGR4 models. (a) All maps, both model and data, weighted equally. (b) Input data weighted by a factor of six while the remaining six models are weighted equally by a factor of 1. In the similarity map, red areas around the periphery showing perfect similarity correspond to ice-free terrain in all inputs.

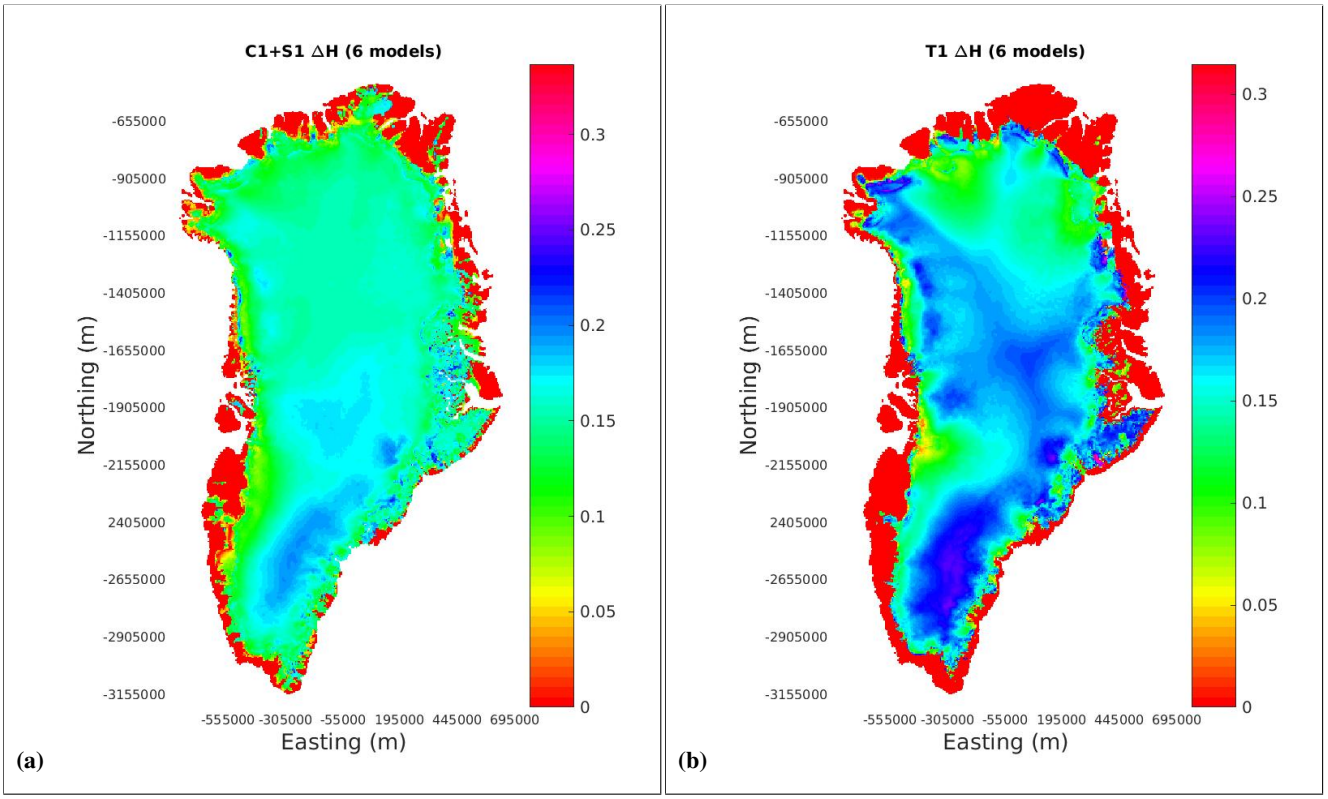

Figure 6. Application of MAPCOMP to investigate combination experiments. We see that results from (a), which compare thickness changes from at the end of the C1 and the S1 experiments, are different from (b), which compares thickness changes at the end of the C1S1 (T1) experiment which combines the perturbations from both the C1 and S1 experiments into a single experiment. Both maps display results from the CSM2, JFA1, JPL2, HSE1, UAF1 and RGR4 models. In the similarity map, red areas around the periphery showing perfect similarity correspond to ice-free terrain in all inputs.

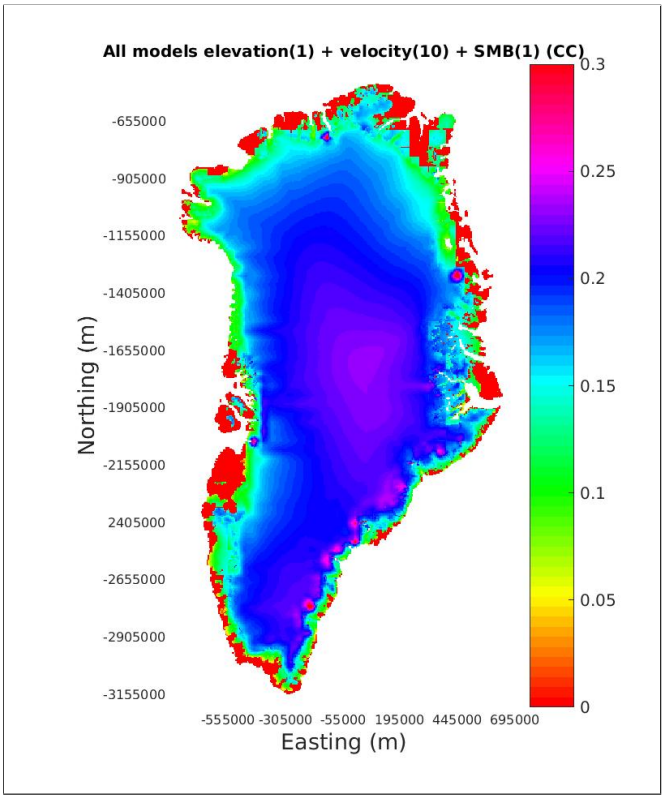

Figure 7. Using MAPCOMP to detect experiment outliers. Comparison of velocity (log-linearly transformed), surface mass balance (standardized linearly), and surface elevation (standardized linearly) of the CC (control) experiment of eight models (CSM2, JFA1, JPL2, HSE1, UAF1, RGR4, WWA1 and WWA2) reveals that one model (WWA1-2) creates artifacts (e.g. the bullseye in the NE and the blocky artifacts in the north). MAPCOMP results clearly show discrepancies from the rest of the experiments. In the similarity map, red areas around the periphery showing perfect similarity correspond to ice-free terrain in all inputs.